Characterization of Bio-oil and Biochar Produced from Co-pyrolysis of Teak Wood Sawdust and Waste Plastic Bottles Using Ablative Pyrolyzer

Article *in* Chemistry Africa · August 2024

DOI: 10.1007/s42250-024-01056-4

CITATIONS
2

READS
61

8 authors, including:

Peter Ikubanni
Bowen University
244 PUBLICATIONS **2,999** CITATIONS
SEE PROFILE

Adekunle Adeleke
Nile University of Nigeria
269 PUBLICATIONS **3,011** CITATIONS
SEE PROFILE

Ayotomiwa Adedayo
Landmark University
2 PUBLICATIONS **2** CITATIONS
SEE PROFILE

Deborah Danjuma
Landmark University
2 PUBLICATIONS **2** CITATIONS
SEE PROFILE

Chemistry Africa
https://doi.org/10.1007/s42250-024-01056-4

ORIGINAL ARTICLE

Characterization of Bio-oil and Biochar Produced from Co-pyrolysis of Teak Wood Sawdust and Waste Plastic Bottles Using Ablative Pyrolyzer

Peter P. Ikubanni[1] · Adekunle A. Adeleke[2] · Ayotomiwa C. Adedayo[1] · Uchechukwu F. Robinson[1] · Deborah E. Danjuma[1] · Olayinka O. Agboola[1] · Timothy A. Adekanye[1] · Oluwasogo L. Ogundipe[1]

Received: 2 February 2024 / Accepted: 6 August 2024

Abstract
The world is gradually moving into renewable energy due to the non-renewability of crude oil. For a sustainable environment and energy generation, co-pyrolysis of biomass and plastic wastes in the environment can be carried out to generate bio-oil and biochar. This study was done to characterize bio-oil and biochar obtained from plastic bottles and sawdust through a fast pyrolysis process using an ablative pyrolyzer. Five different sawdust-plastic compositions (100% sawdust 0% plastic (sample A), 70% sawdust 30% plastic (sample B), 50% sawdust 50% plastic (sample C), 30% sawdust 70% plastic (sample D), and 0% sawdust 100% plastic (sample E)) were charged into the pyrolyzer to obtain bio-oil and biochar. The bio-oil and biochar were characterized using standard methods and equipment. The values for density, pour point, cloud point, viscosity, and pH range from 0.92 to 1.02 g/cm^3, 0.6–1.8^oC, 0.8–2.0^oC, 3.5–7.8 mPa.s, and 3.91–5.26, respectively. Hence, the bio-oil is capable of being useful for energy utilization. For the biochar, the microstructure revealed fibrous rigid structures with pores. The energy dispersive spectroscopy showed that carbon was the main element present, which is the reason for the blackness of the product. Major and minor elements such as K, Mg, Fe, Na, Zn, Cu, Cl, Al, and Ni were observed through the X-ray diffractometer analysis done on the biochar samples. Hence, biochar can be useful for soil improvement and some other applications.

Keywords Sawdust · PET bottles · Biochar · Bio-oil · Waste utilization

1 Introduction

For a sustainable environment, it is important to recycle environmental pollutants and wastes for energy generation [1]. These environmental pollutants and wastes serve as renewable energy sources. Renewable energy sources, such as biomass and wastes, sun, wind, hydropower, geothermal, and marine energies, currently provide 14% of the total global energy demand. Biomass and waste constitute about 12% of the total amount of renewable energy sources [2]. The utilization of renewable energy sources has been driven by the current economic development or challenges, increased energy demand to serve a growing population as well, and increased environmental concerns [3]. Being the only renewable carbon source, biomass is projected to provide a sustainable development role in ensuring proper bioenergy share in the global energy mix [4].

Trinh et al. [5] and Inayat et al. [6] have highlighted that the global production of biofuel benefits from an ample and readily accessible biomass supply. As scientifically established, the origin of biomass is linked to microbes and vegetation [7]. Biomass has various classifications including wood-based, agricultural, forestry, municipal and industrial waste, food waste, and animal and human-generated waste [6, 8, 9]. The transformation of biomass into bioenergy could either be by biological, chemical, or thermochemical conversion technology [3, 10–12]. As a result of the disadvantages of biological and chemical conversion technologies [6], thermochemical conversion technology is in the limelight for chemical and fuel molecule production [3].

Out of the thermochemical technologies, pyrolysis has been explored in bio-oil production, which is further

✉ Peter P. Ikubanni
ikubanni.peter@lmu.edu.ng

[1] Department of Mechanical Engineering, Landmark University, Omu-Aran, Nigeria

[2] Department of Mechanical Engineering, Nile University of Nigeria, FCT, Abuja, Nigeria

Published online: 21 August 2024

processed and refined to produce biofuels [6, 13]. These biofuels produced via pyrolysis are more advantageous when compared to fossil fuels because sulfur and nitrogen emissions are limited during fuel production [13, 14]. Aside from the bio-oil produced during pyrolysis, other products that are generated include biochar and syngas, with various application options. The core configurations of lignocellulosic biomass are cellulose, hemicellulose, and lignin [15]. These compositions are key in biomass utilization for bio-based chemicals and polymers [6, 16]. Bio-oil is acidic, polar, and viscous due to its complex composition; hence, hindering its direct utilization [6, 17]. Hence, the bio-oil is required to be upgraded via steam reforming, catalytic cracking, and hydrotreating [18]. The processes involved in the upgrading of bio-oil are of high cost.

As reported by Inayat et al. [6], 60% of the global plastic production of 367 million metric tons finds their way into landfills. These are environmental wastes that can be converted into bio-energy. Hence, plastic pyrolysis can help to produce hydrogen-rich diesel-grade hydrocarbon fuel [19]. For the transfer of hydrogen from the hydrogen-rich feedstock of plastic to the oxygen-rich feedstock of biomass, a co-pyrolysis idea was conceived. The upgraded bio-oil obtained occurs through the hydrogenation and hydrodeoxygenation reaction [6]. Depending on the parameters utilized, it is germane to understand the key parameters that could affect the bio-oil and biochar yield during a co-pyrolysis process. Some of the pyrolysis parameters that could affect bio-oil and biochar are heating temperature, heating rate, residence time, and the size of the biomass particles [20]. Based on the findings of Tang et al. [21] and Dorado et al. [22], the ratio of plastic-to-biomass plays a significant influence on the yield and quality of the product.

Numerous scholars have converted diverse biomass materials into bio-oil, biochar, and syngas using fast and slow pyrolysis in their investigations [23–30]. Several studies have been done on the pyrolysis of plastic and biomass for bio-oil and biochar production. Saleem and Baig [1] produced bio-oil and biochar from four different biomass using the conventional pyrolysis technique in a fixed bed reactor. The products obtained were further characterized to obtain the highest bio-oil and biochar yield. The effects of temperature variation (300, 400, and 500^oC) and heating rate (3.69 ^oC/min) on the bio-oil and biochar yield were evaluated. The rate of reaction was enhanced using sulfuric acid. Bio-oil yield increased with temperature increased while biochar yield increased at lower temperatures. Adegoke et al. [31] designed an ablative pyrolyzer which was tested using plastic and biomass. The bio-oil and biochar produced were characterized. The bio-oil was found useful for energy usage. Alabdrabalnabi et al. [3] used machine learning to estimate the biochar and bio-oil yields during the co-pyrolysis of biomass and plastics since it is crucial to forecast the yields of both products. Through the study, important phenomena of the co-pyrolysis of biomass and polymers were gained. The multi-waste biomass co-pyrolysis for the production of bio-oil was carried out by Mariyam et al. [13]. Fast pyrolysis was employed in the study to generate high bio-oil yields. The influence of single, binary, and ternary pyrolysis of feedstock on the thermal degradation behaviour and bio-oil composition were investigated using a Pyroprobe reactor.

Although numerous studies have been carried out on the pyrolysis of biomass and polymers using sophisticated techniques and equipment, a new locally made ablative pyrolyzing equipment was developed to achieve pyrolysis of waste biomass. It is imperative to consider co-pyrolysing sawdust and PET bottles in a newly fabricated thermochemical device. Due to the heating chamber of the device, the size of the PET bottles was minimized to achieve the required yield of the bio-oil. Therefore, this study characterizes bio-oil and biochar produced through the co-pyrolysis of plastics (PET bottles) and sawdust at different mix ratios using an ablative pyrolyzer. With the characterizations, bio-oil upgrading could be effectively established to acquire valuable and quality liquid fuel. The physicochemical properties of the obtained bio-oil product such as colour, odour, density, viscosity, pour point, cloud point, and pH value were characterized. The functionality of the bio-oil was determined using Fourier Transform Infrared (FTIR) technique; while the biochar was characterized to determine the phase structure and internal morphology using an X-ray diffractometer (XRD) and scanning electron microscope, with an attachment of energy dispersive spectroscope (SEM-EDS) respectively. The characterizations done on the biochar are to ascertain its applications in soil pollutant removal. The elemental and structural analyses assist in determining the effect of biochar on the environment.

2 Materials and Methods

2.1 Materials

The materials used in this study include Polypropylene terephthalate (PET) plastic waste bottles and sawdust. The PET waste bottles (Fig. 1a) were collected within the premises of Landmark University, Omu-Aran, Nigeria (Latitude: 8° 08’ 18.85” N, Longitude: 5° 06’ 9.36” E). The sawdust was obtained from a local sawmill in Omu-Aran, Kwara State (Fig. 1b). A test rig (an ablative pyrolyzer) was used to pyrolyze the wastes.

Fig. 1 (**a**) PET Bottle Fig. 1(**b**) Sawdust particles

Table 1 Experimental design of the pyrolysis process

Designation	Sawdust (wt%)	PET bottle (wt%)	Heating temperature (^oC	Heating rate ^oC/(min
A	100	0		
B	70	30		
C	50	50	450	5
D	30	70		
E	0	100		

2.2 Sample Preparation and Characterization

The PET bottles were cut into small pieces (50 mm by 10 mm size) before being washed twice with detergent to remove dirty particles and oil. It was then rinsed with clean water. Then, it was dried in open air for three days. The sawdust (50 µm size) was sundried for five days (6 h/day) to reduce moisture. The shredded PET bottles and the sawdust were then packed in separate air-tight containers and kept for further work on them.

The ultimate analysis of the raw sawdust and PET bottle is necessary to determine the carbon, hydrogen, oxygen, nitrogen, sulfur, and ash contents. The LECOCHN 2000 Elemental Analyzer was used to determine the carbon, hydrogen, and nitrogen contents of the feedstocks following the ASTM D5291-02 standard. However, the oxygen content was determined by the difference. LECO SC-432DR apparatus was used to obtain the sulfur content based on ASTM D4239-83 standard. The proximate analysis to determine the moisture content (MC), volatile matter (VM), and ash content (AC) was done using a muffle furnace (LF3/F4244 Model, Vecstar Ltd., United Kingdom) based on ASTM D3173, ASTM D3175, and ASTM D3174 standards, respectively. The fixed carbon (FC) content was evaluated by difference.

2.2.1 Mixing Ratio of the Sawdust and PET Bottles

The mixing ratios of the sawdust and PET bottles for the pyrolysis experiment in the ablative pyrolyzer are presented in Table 1.

2.2.2 Pyrolysis of the Plastic and Biomass

A developed ablative pyrolyzer was used as the test rig for the pyrolysis. The ablative pyrolyzer is used to create fuel from a mixture of waste plastic and biomass in specific ratios as presented in Table 1. In this method, the mixture of plastic with biomass was heated up to 450^oC at a heating rate of 5 ^oC/min [32] in the absence of oxygen in a reactor. The mixture reaches its melting point and melts, and the vapor rises to the surface, where it is collected in the condensing unit. The condensable vapor is then condensed using water. Plastic and biomass co-pyrolysis results in the obtaining of liquid (bio-oil) and solid (biochar) products. The steps involved in processing the raw materials into bio-oil and biochar are illustrated in Fig. 2. The cooling protocol adopted is to alloy the ablative to cool naturally after each run.

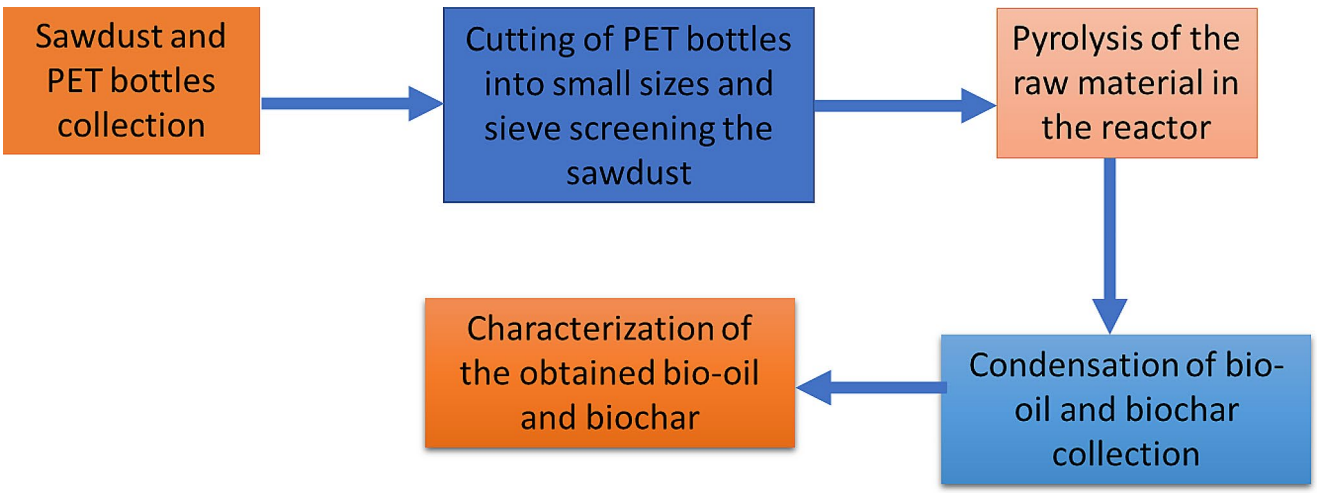

Fig. 2 Steps involved in obtaining the products

The processes involved in the pyrolysis of the biomass and plastic to obtain the bio-oil and biochar are shown in Fig. 2.

Feeding the already chopped small pieces of waste plastic and sawdust into the reactor at the specified ratios was done manually. Biomass (sawdust) and plastic were combined in a specific ratio after the plastic had been cut into small pieces (50 mm by 10 mm). The mixture was dried before feeding into the pyrolysis reactor. The pyrolysis reactor in this method was a cylindrical chamber. The reactor was placed inside an electric heater band. The heater has a 3.6 kW capacity and is insulated with glass wool. A vacuum was created inside the reactor by using high temperatures outside the reactor. A sensor is located within the reactor which is coupled to a temperature controller that regulates the temperature inside the reactor. The procedure was carried out inside the reactor at a temperature of about 450^oC at a heating rate of 5^oC . The pyrolysis products were sent to a water-cooled condenser, where the condensed liquid was collected and stored for further analysis. The experimental runs were done in triplicate. The experimental setup of the method is depicted in Fig. 3. The bio-oil obtained was in its most basic form while the biochar was collected after the reactor was cooled to room temperature.

2.2.3 Bio-oil Yield

A weighing balance (Serial No: 8731323543) was used to obtain the mass of the bio-oil and biochar produced from the wastes used in the pyrolysis process. The bio-oil and biochar percentage yields were determined using Eqs. (1) and (2), respectively.

$$\%Bio-oil\ yield = \frac{m_b}{m_s} \times\ 100 \tag{1}$$

$$\%Biochar\ yield = \frac{m_c}{m_s} \times\ 100 \tag{2}$$

where the mass of the bio-oil yield is m_b (g), the mass of the sample (waste biomass and PET bottle) is m_s (g), and the mass of the biochar yield is m_c (g).

2.3 Physicochemical Properties of the Bio-oil and Biochar

The density of the bio-oil produced through the ablative pyrolyzer with the hybrid mixture of sawdust and PET bottles was obtained by measuring the volume of the bio-oil in a volumetric cylinder and measuring the mass of the same volume of bio-oil in a density tube by using the analytical weighing balance. The density was then determined

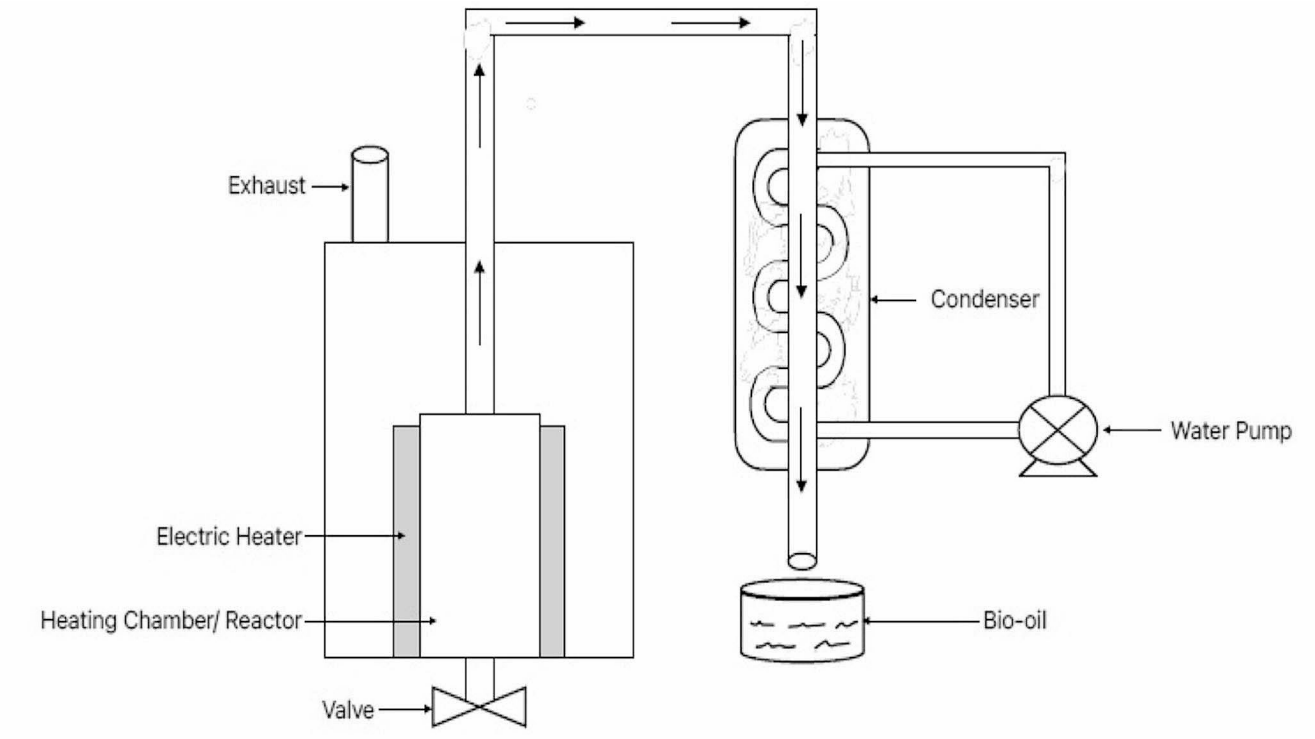

Fig. 3 Experimental setup

by Eq. (3). The pH of the produced bio-oil was obtained by dipping a pH meter (PHS-550, Sinotester Co. Ltd., China) probe into the test bio-oil liquid and the value displayed on the meter was recorded as pH value. The viscosity of the bio-oil generated was obtained using a viscometer (Serial No: 0600414248) following the ASTM D445 standard procedure. Equation (4) was used in the evaluation of the viscosity of the oil, according to Adegoke et al. [31]. The pour and cloud points of the bio-oils were obtained using a Cryostat according to the recommendation of Khan et al. [19], which measures up to $-35^{o}C$. The Fourier Transform Infrared (FTIR) spectroscopy analysis of the bio-oil samples was obtained using the Perkin Elmer FTIR Spectrometer 1725X (Perkin Elmer Inc., USA) having a scan range of 4000–650 cm^{-1} at a resolution of 8 cm^{-1}. The necessary procedures as reported by Adegoke et al. [31] were adopted for the FTIR analysis. For the X-ray diffraction (XRD) analysis, the PANalytical Empyrean diffractometer (Malvern Panalytical Ltd., UK) was used to characterize the biochar's phase structure and determine its crystallinity. The X-ray diffractometer has a scan range of 2θ = 4–70° and a scan speed of 0.026°/min, and its Cu K radiation is 1.5406 at an acceleration voltage of 45 kV and current of 40 mA. Using the X'Pert Highscore Plus software connected to the PANalytical diffractometer, the acquired peaks were matched with the mineral phases.

$$Density\ \left(\frac{g}{cm^3}\right) = \frac{mass\ (g)}{volume\ (cm^3)} \tag{3}$$

$$Viscosity = Time\,(s) \times\ 0.10\,(viscosity\ constant) \tag{4}$$

2.4 Microstructural Analysis of the Biochar

Using a scanning electron microscope (Vega 3 Tescan Model, Tescan Group, Czech Republic) with an energy-dispersive X-ray analyzer (EDX) attachment and high vacuum (HV) mode at 20 kV accelerating voltage, the samples' microstructural pictures were captured. The EDX was employed to perform bulk elemental analyses of the biochar.

Table 2 Proximate and ultimate analysis of the sawdust and PET bottles feedstock

Ultimate analysis			Proximate analysis		
Component	Content (%)		Component	Content (%)	
	Sawdust	PET Bottle		Sawdust	PET Bottle
C	49.27	63.90	MC	3.90	–
H	5.83	4.20	VM	79.01	83.7
N	1.05	0.32	FC	13.87	26.3
O	43.77	31.20	AC	3.20	–
S	0.08	0.08			
HHV	20.57	23.52			

3 Results and Discussion

3.1 Raw Sawdust and PET Bottles Characterization

The ultimate and the proximate analysis of the feedstocks (sawdust and PET bottles) are presented in Table 2. Table 2 shows that there is high energy content in both the sawdust and the PET bottles. Hence, it is suitable for bio-oil production. The result of the HHV revealed that the PET bottle has a higher energy content than the raw sawdust. The table revealed that both feedstocks were predominantly composed of volatile matter and fixed carbon. The PET bottle had a higher VM and FC than the sawdust. Although sawdust is combustible, the presence of moisture content could affect its energy content compared to PET bottles. There is no record of MC and AC detected in the PET bottle feedstock. The high VM of the PET bottle over the sawdust feedstock could be linked to the high HHV of the PET bottle feedstock. Hence, the PET bottle at high temperature would devolatilize faster than the sawdust. The devolatilization process enhances the feedstock to produce more bio-oil yield and burn gases in the reactor [33]. The amount of impurities remaining after biomass combustion is known as ash content, which was obtained to be 3.20%. This relatively low value ensures the usability of the sawdust for the pyrolysis process. It also ensures a high bio-oil yield. A high AC is very detrimental to the reactor because there is a high risk of increased slag formation, deposition of harmful substances, fouling, and corrosion phenomenon [34]. The ultimate analysis of both feedstocks revealed carbon and oxygen to be high compared to other elements such as hydrogen, nitrogen, and sulfur. The presence of high carbon and moderate hydrogen contents reveals that the feedstocks would produce hydrocarbons during the pyrolysis process. Low nitrogen and sulfur content reduce the risk of releasing harmful gases such as NO_x and SO_x into the environment.

3.2 Physical Appearance of the Bio-oil and Biochar

Fi]g. 4(a) represents the bio-oil obtained from the sample composition, while Fig. 4(b) displays the biochar product obtained from the pyrolysis process. The coloration of the bio-oil was dark brown (Fig. 4(a)). The dark-brown coloration could be attributed to the heavier component of the carbon present in the bio-oil [25]. The colour of the biochar of all the samples was black (Fig. 4(b)), while the bio-oil had a pungent smoky odour. Carbonization of the samples which leads to devolatilization of the lignin content, which has high carbon content, could have led to the biochar coloration [34]. The biochar of all the samples was agglomerated and coarse; however, the biochar of samples D and E clogged as a result of the abundant plastic in the mixture

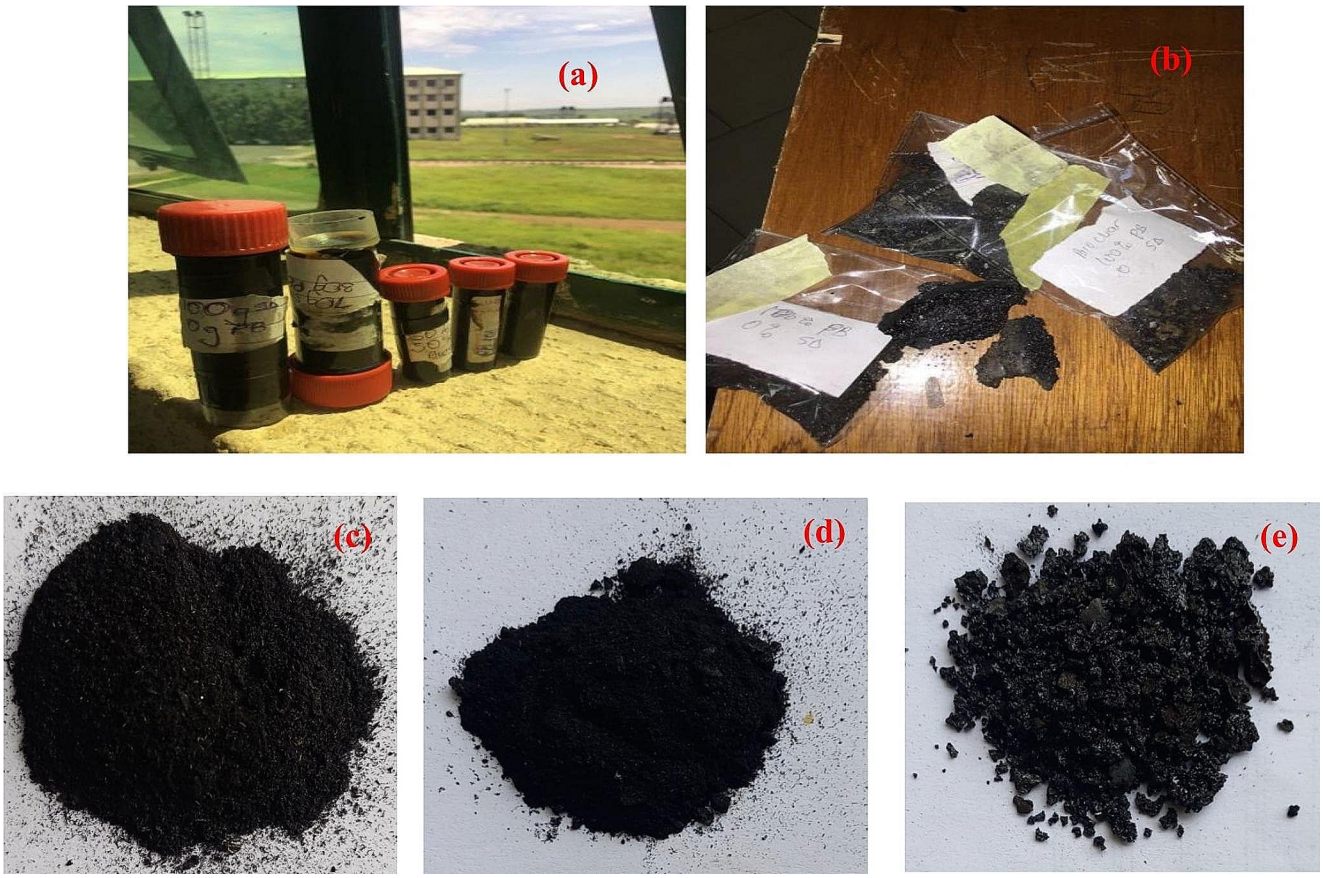

Fig. 4 Products obtained (**a**) Bio-oil (**b**) Biochar (**c**) Biochar of 100% Sawdust (**d**) Biochar of 50% Sawdust and 50% Plastic (**e**) Biochar of 100% Plastic

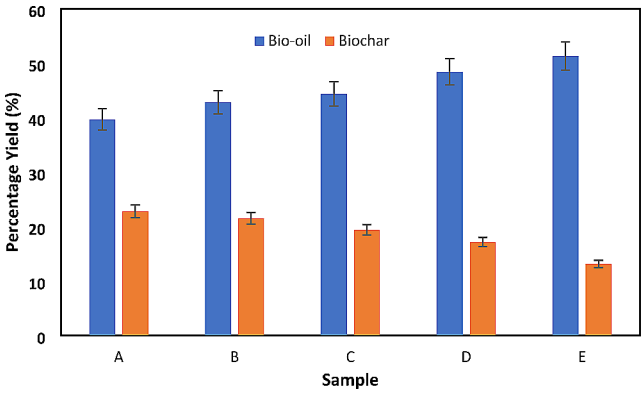

Fig. 5 Percentage yield of the bio-oil and biochar

poured into the heating chamber of the reactor. The fineness of the biochar reduced as the plastic quantity increased while the sawdust quantity reduced in the mixture of the sample (Fig. 4(c)– (e)).

3.3 Bio-oil and Biochar Yield

It can be observed from Fig. 5 that the highest amount of bio-oil (51.33%) was obtained with sample E (100% plastic), while the least (39.72%) was at sample A (100% sawdust). Furthermore, it can be observed that as the amount of plastic increased in the mixture, the bio-oil yield increased. The biochar yield decreased with an increase in plastic in the composition of the samples. However, the 100% plastic (Sample A) had the least biochar yield (13.16%) while sample A showed the highest biochar yield (22.82%). Biomass lignin decomposition results in biochar generation. The low biochar obtained in sample E could be attributed to heat energy generated in converting the biomass into more bio-oil. The plastic yielded more bio-oil through the pyrolysis process; hence, resulting in low biochar yield at 450^oC . Maximum bio-oil was produced from the plastic pyrolysis with clogging biochar due to the pyrolysis temperature used during the experiment.

In the study of Egbosiuba [20], the effect of temperature and heating rate on cassava peel's bio-oil was evaluated. The maximum bio-oil yield was 24.35%, which was obtained at a temperature of 600 ^oC and 10 ^oC/min heating rate. The bio-oil yield of the study was lower than the obtained yield in this present study. The increase in temperature positively influences bio-oil yield. The bio-oil yield from *L. leucocephala* pyrolyzed in a fluidized bed reactor

Table 3 Bio-oil properties obtained from 100% sawdust and 100% PET

Properties	100% Sawdust bio-oil	100% PET bio-oil
Carbon (%)	43.47	62.53
Hydrogen (%)	7.22	8.24
Nitrogen (%)	0.71	0.55
Sulfur (%)	0.24	0.06
Oxygen (%)	48.36	28.62
H/C molar ratio	0.17	0.13
O/C molar ratio	1.11	0.46
Heating value (MJ/kg)	24.23	35.57

showed that the highest bio-oil yield value was 50.25% at 500^oC temperature. Lowering fluidization gas reduced the bio-oil yield to 48.50% at the same temperature [35]. More bio-oil and less biochar were obtained from the pyrolysis of *S. japonia* biomass in a fixed-bed reactor [36]. This was the phenomenon observed for the samples in this present study. The bio-oil yield of the biomass was 48.4% at a temperature of 450^oC while at higher temperatures, the bio-oil yield reduces. It was further reported that an increase in temperature above 450^oC resulted in a reduction of bio-oil yield in the study of Chukwuneke et al. [37]. A high bio-oil yield of 69.5% at 450ºC was obtained in the fixed bed reactor used. Secondary reactions of the compounds with heavy molecular weight in the pyrolysis vapours [37]. The quantity of biochar is always lower than the bio-oil [20, 37]. However, it has been reported by several studies that biochar yield tends to reduce with an increase in pyrolysis temperature [35, 36]. During the co-pyrolysis of PET and woody biomass for the production of bio-oil in a fixed bed reactor, Anandaram et al. [38] observed that the maximum bio-oil yield was 40.5% at 450^oC for the pure woody biomass while the biochar yield was about 24% at 550^oC. Pure PET maximum bio-oil yield was obtained at 500^oC. The high yield of the bio-oil from PET could be linked to the breakage of the stability of C = C bonds of polymeric materials at higher temperatures [38, 39]. Furthermore, the bio-oil yield of the PET bottle was obtained between 48 and 55% for a temperature range of 350 to 550^oC. More bio-oil was obtained with the increased temperature. The co-pyrolysis result revealed that more bio-oil content is generated as the content of the PET bottles increases in the mixture of the biomass. This phenomenon was linked to the presence of polyolefin polymers which serve as a hydrogen donor during pyrolysis to produce radical interaction to form optimum bio-oil. PET is known to contain maximum volatiles compared to biomass [38]. Invariably, the biochar yield decreased with the increase in PET quantity in the composition. These observations are witnessed in this present study. The bio-oil yields increase and biochar yields decrease with an increase in the quantity of PET bottles.

Table 4 Density of the bio-oil yield

Sample	Density (g/cm^3)
A	1.02
B	0.98
C	0.96
D	0.94
E	0.92

Pyrolysis was done at a temperature of 450^oC, which is regarded as a temperature that classifies the process as fast pyrolysis. As a result of the rapid degradation of the biomass, gaseous products are produced. Consequently, the transition from gas to liquid happens more swiftly [40]. Thus, the bio-oil yields entering the condenser exhibit an accelerated rate.

The bio-oil obtained from the 100% sawdust and 100% PET were characterized to determine their elemental compositions and heating values as presented in Table 3. The carbon and hydrogen contents of the bio-oil increased from 100% sawdust bio-oil (43.47%) to 100% PET bio-oil (62.53%) while that of oxygen content reduced from 48.36% (100% sawdust bio-oil) to 28.62% (100% PET bio-oil). The reduction of the oxygen content is reported to improve the heating value of the bio-oils [38]. Anandaram et al. [38] observed that as the PET quantity increased when co-pyrolyzed with woody biomass, the carbon and hydrogen contents increased with decreased oxygen content. This implies that as the PET quantity increases, the oxygen content reduces with an increase in the HHV of the bio-oil produced. More so, the lower the sawdust quantity in the co-pyrolyzed mixture, the lower the oxygen content present in the bio-oil produced. Therefore, for effective and higher HHV bio-oil generation, woody biomass (sawdust) with PET can be co-pyrolyzed. The HHV of the 100% sawdust and 100% PET were 24.23 and 35.57 MJ/kg, respectively.

3.4 Physicochemical Properties

3.4.1 (a) Density

The density values of the samples used for the study are presented in Table 4. The density of the samples A to E range from 1.02 to 0.92 g/cm^3. From Table 4, it can be observed that, as the quantity of sawdust decreases with PET increase in the mixture, the density of the sample decreases. The combustion performance of fuel is significantly influenced by its density, which is a fundamental physical property. Density relies on the atomic mass of the constituent compounds comprising the substance. Consequently, if the volume remains constant, a higher density will result from greater atomic masses of the constituent compounds [41]. Although the amount of bio-oil yield obtained from sample

E is much compared to sample A, the density of the bio-oil differs. Sample A exhibits the highest bio-oil density while sample E has the lowest. The higher the plastic material in the mixture of the biomass materials used in the bio-oil generation, the better the density of the bio-oil produced. According to ASTM D975, the density of a conventional diesel is between 0.815 and 0.870 g/cm^3.

3.4.2 (b) Pour Point and Cloud Point

The pour point and cloud point values of the samples used for the study are presented in Fig. 6. The results of the pour point of samples A to E range from 0.6 to 1.8^oC, while the cloud point of samples A to E range from 0.8 to 2.0^oC. The pour point is the lowest temperature at which a fluid can flow [42]. Lower pour point values indicate better flow properties at lower temperatures. Figure 6 revealed that sample A (100% sawdust) has the highest pour point value (1.8^oC), indicating poorer low-temperature flow properties. The higher pour point temperature of the bio-oil obtained from the pyrolysis of 100% sawdust can be attributed to several factors such as the composition of sawdust. Sawdust primarily consists of cellulose, hemicellulose, and lignin [43]. These higher molecular weight compounds tend to have higher melting points, leading to an elevated pour point temperature [44].

The cloud point measurement refers to the temperature at which a noticeable quantity of solid phase starts to form during cooling within the timeframe of the measurement, under specific pressure conditions. This temperature is influenced by factors such as the composition of the oil, the measurement method employed, the thermal history of the sample, the timing of the measurement, and the fluid properties associated with crystal nucleation and growth. The cloud point followed the same trend as the pour point. The value of the cloud point was found to be higher compared to the pour point. Hence, sample A being the highest of all suggests that it would start to form a solid phase faster when cooled.

3.4.3 (c) Viscosity

The viscosity values of the bio-oil obtained in this study are displayed in Fig. 7. The results of the viscosity of samples A to E ranged from 7.8 to 3.5 mPa.s measured at a temperature of 25^oC. When it comes to bio-oil treatment, viscosity stands out as the key factor influencing the treatment temperature. It can be observed that sample A has the highest viscosity while sample E has the lowest viscosity. Based on the obtained viscosity result, the trends of values are sample A > sample B > sample C > sample D > sample E. Sample A's high viscosity may be explained by the fact that bio-oil

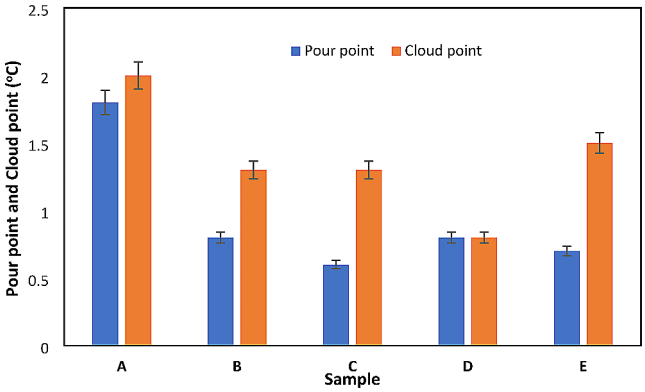

Fig. 6 Pour point and cloud point

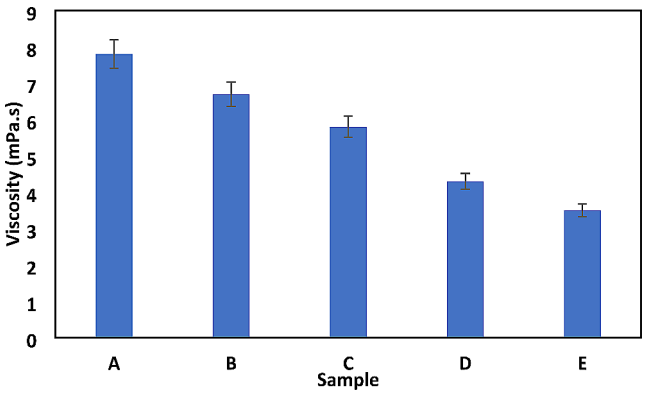

Fig. 7 Viscosity of the bio-oil

derived from biomass always has a higher viscosity than bio-oil derived from fossil fuels [31]. The viscosity of the bio-oil obtained from rice husk was 5.57 mm/s^2 as reported by Li et al. [45], while Anandaram et al. [38] obtained 7.1 and 4.1 cst for woody biomass and PET bottles, respectively. The viscosity of bio-oil obtained from rapeseed cake is 38 cSt at 50^oC as reported by Ozcimen and Karaosmanoglu [46]. The viscosity of the bio-oil obtained in this study finds a correlation with the study of Anandaram et al. [38]. However, the viscosity for conventional diesel is reported to be 2.0 to 4.0 cst at 40^oC (diesel) according to ASTM D975 and 180 cst for heavy fuel. For standard heating oil (Code 615) and Fuel oil (Code 670), the viscosity is 54 and 65 cst, respectively [46].

3.4.4 (d) pH Determination

The pH of the bio-oil generated from each sample composition was analyzed. It can be observed that all the bio-oils obtained from the biomass are acidic. The pH is low and ranges from 3.91 to 5.26. The pH value of the pyrolysis oil is dependent on the feed material. As observed from the results of the pH determination presented in Table 5, sample A is the most acidic with a pH value of 3.91 while sample

Table 5 pH value of bio-oil

Sample	pH
A	3.91
B	3.92
C	4.16
D	4.50
E	5.26

E is the least acidic. The high acidity of sample A can be attributed to the hydrocarbons present in the components such as cellulose, hemicellulose, and lignin contents in wood biomass [47]. During fermentation, these hydrocarbons become acidic with various organic reactions occurrence. Hence, the acidic value of samples B to D reduces as the plastic content in the mixture increases.

3.5 SEM-EDS of the Biochar

In the adsorption process, the surface morphology and surface porosity are important features [48]. The micrographs of the biochar from samples A, C, and E, are displayed in Figs. 8, 9 and 10. The micrograph of sample A shows that the biochar of sawdust (100%) has the presence of numerous pores on the surface (Fig. 8(a)). This same observation was reported by Ma et al. [49] when corncob was characterized. Many pores and cracks were observed on the surface and profile of the sample. The sawdust biochar has a fibrous rigid structure. Pores were produced because of the volatilization of the organic matter present. However, the numerous pores were reduced and a completely different structure or appearance was observed on the surface of the biochar obtained from sample C (Fig. 9(b)). The structure obtained could be linked to the addition of the plastic material which was pyrolyzed with the sawdust at the same mix ratio. Figure 10(a) showed an entirely different morphology, with minimal pores as a result of the clogging of the plastics after carbonization. Ridge-like structures were observed on the morphology of the biochar due to the production of tars that filled the micropores as well as other decomposed materials that blocked the pores [50, 51].

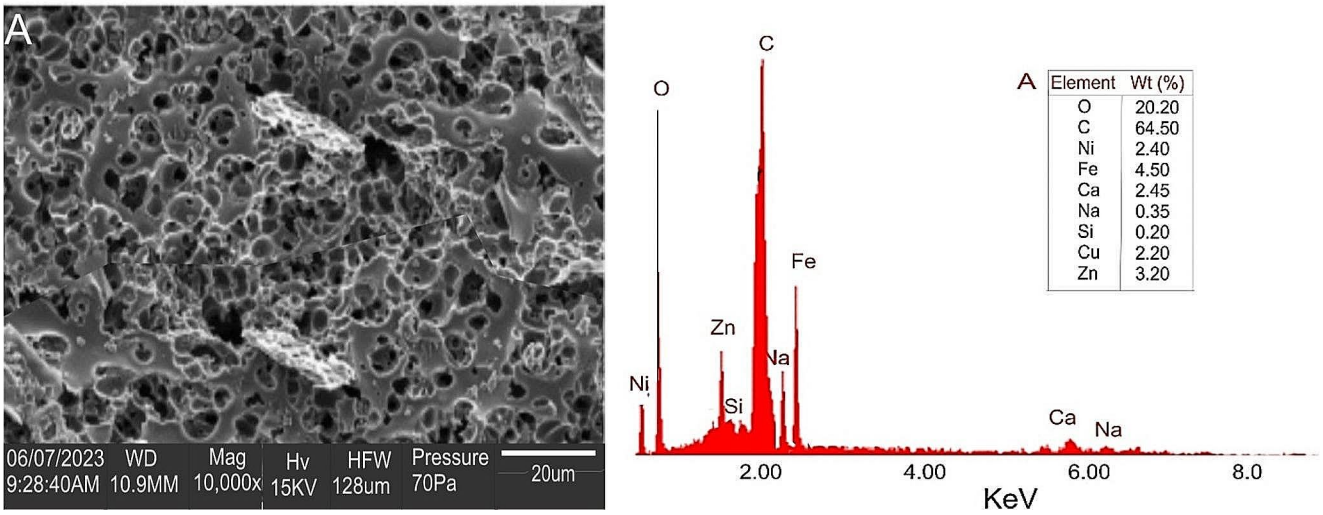

Fig. 8 SEM-EDS of biochar obtained from 100% sawdust

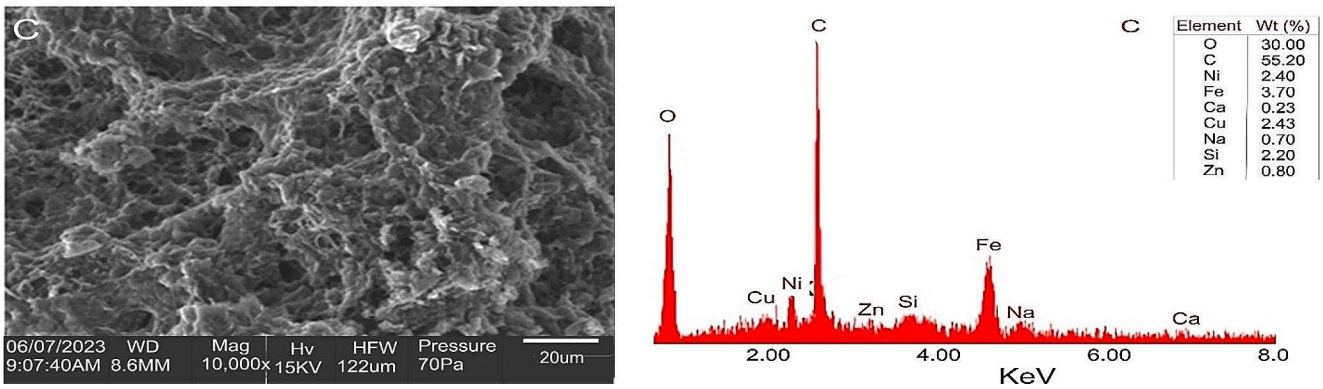

Fig. 9 SEM-EDS of biochar obtained from 50% sawdust:50% plastic

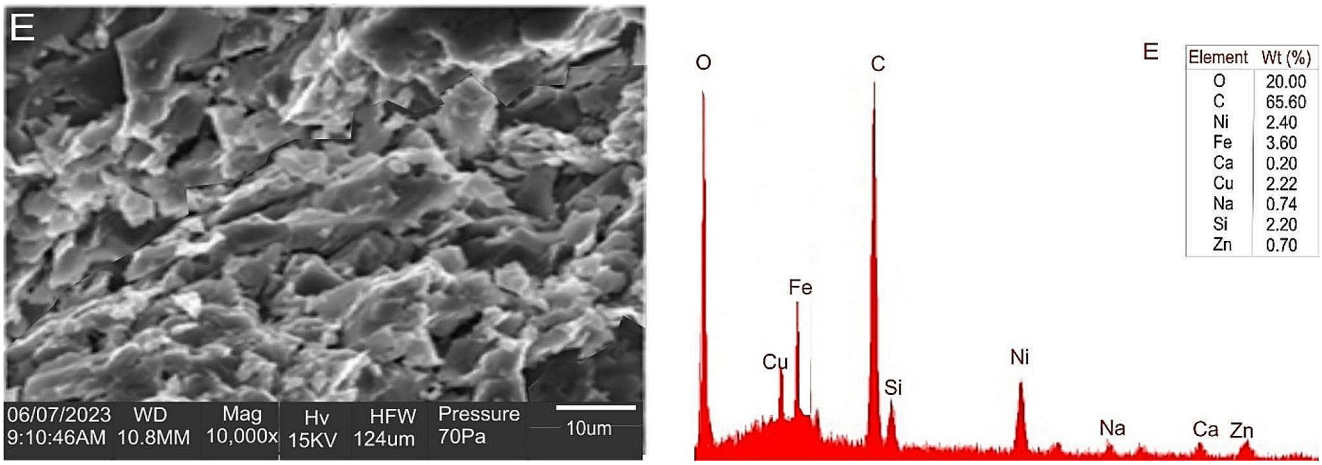

Fig. 10 SEM-EDS of biochar obtained from 100% plastic

The EDX spectra of samples A, C, and E revealed that carbon has the highest content (Fig. 8(b), 9(b), and 10(b)). This is attributed to the carbonization process of the biomass and plastic wastes. During the carbonization process, volatile matter is released through the pyrolysis process while the lignin present in the sawdust particles undergoes degradation. Devolatilization of the wastes in the pyrolysis reactor resulted in bio-oil and biochar production. The black colour of the biochar was due to the carbonization of the product. More so, the dominance of carbon in the EDX spectra of all the biochar samples is a confirmation of the decomposition of the cellulose, lignin, and organic matter present in the biomass and plastic wastes [48].

Aside from the high carbon content in the biochar, a significant amount of oxygen was observed in each biochar sample. It can be said that the oxygen content originates from the -COO and -OH functional groups existing on the surface. The presence of the elemental constituents of the biochar indicates a good bonding between silicon and carbon. Hence, further thermal treatment of the biochar in a muffle furnace at a high temperature ($1200^{o}C$) to become ash would lead to the formation of SiC, which can be detected using the X-ray powder diffraction (XRD) technique [45]. Other metals such as Zn, Cu, Fe, and Na have a great tendency to become strengtheners as reinforcing materials in metal matrix composites when combined with oxygen to become oxides of the metals [52–55]. The functionality of each of the metal oxides has been documented elsewhere [52]. More so, the metals present in the spectra are good macro- and micro-elements for soil improvement and plant growth.

From the EDX spectra, the O/C ratio for samples A, C, and E, was 0.313, 0.543, and 0.305, respectively. The ratio provides information about the quantity and polarity of surface functional groups in the biochar that contain oxygen.

3.6 FTIR Analysis of the Bio-oil

A representative FTIR spectrum of the bio-oil sample is displayed in Fig. 11, which was used to identify the functionality (functional groups) of the bio-oil sample. Table 6 highlights the peak, compound, and functional groups for all the samples. The spectra of the bio-oil samples A, B, and D revealed a peak that hovers around 3600–3000 cm^{-1}. The peak around this range is considered to be the stretching and bending of OH vibration. This implied that water molecules are present in the bio-oil obtained [31]. However, this peak was not detected in the 100% PET bottle bio-oil sample. At these peaks, the presence of -OH stretching is noted. This implied the existence of α-Hydroxy acids as well as water molecules. The molecules are volatilized at a higher temperature. Hence, biomass aromatization is increased with increased temperature which enhances dehydration [51, 56]. The FTIR of the bio-oil samples that have the presence of sawdust revealed similar peaks and functional groups. However, there are more peaks detected between 1800 and 650 cm^{-1} range for the 100% sawdust bio-oil sample (Sample A) compared to the bio-oil samples in Samples B and C, which contain the mixture of sawdust and PET bottles.

The peak at 2967 cm^{-1} (Table 6) indicates a symmetric and asymmetric stretching vibration of C-H in the CH_2 functional group. A carbonyl functional group was detected between 1730 and 1700 cm^{-1} of the 100% sawdust bio-oil sample (Fig. 11). The C=C stretching bond linked to the production of more oil yield was detected. Other compounds and functional groups detected are displayed in Table 6. Generally, based on the presence of the functional groups detected, these bio-oil samples contain alcohols, acids, and esters. The esterification process can be further carried out on the bio-oil yield to make it useful for energy generation. The presence of the combinations of either two or three of C, H, and O elements within the biomass confirmed that

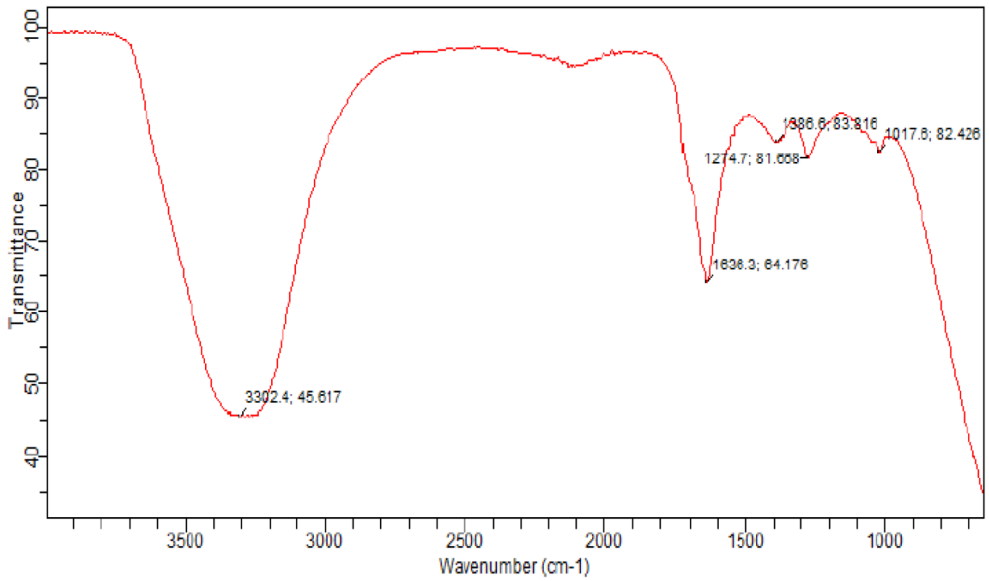

Fig. 11 Representative FTIR spectrum for bio-oil

Table 6 FTIR analysis of bio-oil samples

Sample	Wave number (cm^{-1})	Compound	Functional group
A	3350.9	OH stretching	Alcohol, Phenols
	2967.0	C-H stretching	Alkenes
	1699.7	C = O stretching	Carbonyl
	1518.3	N-O asymmetric stretching	Nitro compound
	1453.7	C-H bending	Alkanes
	1267.3	C-O stretching	Carboxylic acids, Esters, Ether
	1114.5	C-O stretching	Carboxylic acids, Esters, Ether
	1021.3	C-O stretching	Ether
B	3302.4	OH stretching	Alcohol, Phenols
	1636.3	C = C stretching	Alkenes
	1386.6	C-H bending	Aldehyde
	1274.7	C-O stretching	Alkyl Aryl Ether
	1017.8	C-O stretching	Ether
C	3291.2	OH stretching	Alcohol, Phenols
	1640	C = C stretching	Alkenes
	1397.8	C-H bending	Alkanes
	1274.7	C-O stretching	Alkyl Aryl Ether
	1017.6	C-O stretching	Ether
D	3067.8	C-H stretching	Alkenes
	2903.2	C-H stretching	Alkanes
	2549.5	C-H stretching	Thiol
	1684.8	C = O stretching	Conjugate Ketones
	1602.8	C = C stretching	Unsaturated Ketones
	1479.8	C-H bending	Alkanes
	1453.7	C-H bending	Alkanes
	1410.4	OH bending	Carboxylic acids
	1360.5	OH bending	Alcohol, Phenols
	1263.6	C-O stretching	Alkyl Aryl Ether
	1177.8	S = O stretching	Sulfonate
	1069 – 1025	C-O stretching	Vinyl Ether
	935 – 710	C = C bending	Alkenes

cellulose, hemicellulose, and lignin are present. According to Shaaban et al. [57], the synthesis of biochar through lignocellulosic degradation is a free radical process. This process initiation occurs with the cleavage of bonds among the biomass structural oxygen and inorganic components via thermal hemolytic phenomenon.

3.7 XRD Analysis of the Biochar

The characterization of the biochar via XRD analysis is important to understand the presence of different crystalline materials that would influence the biochar properties for its applications. Figure 12 (a)– (e) display the XRD spectra of the biochar samples obtained from the ablative pyrolyzer. The present spectra suggest that most of the crystalline regions present in the biochar are linked to cellulose crystallinity. The peaks corresponding to the formation of turbostratic carbon crystallites within the biochar's structure were detected around 42°– 44°. However, the turbostratic crystallites were very limited in the structure. The quantitative analysis reports of the XRD displayed various mineral phases from the structure of the biochar. The potential formation of graphene can be linked to the presence of graphite, an allotrope of carbon. This is a unique structure that finds placement within the amorphous carbon and crystalline graphite phases [48]. The common mineral phases present in all the biochar samples are silicon oxide, graphite, osumilite, chlorite, and albite. The major constituent elements in osumilite are Potassium (K), Sodium (Na), Iron (Fe), Aluminum (Al), and Silicon (Si).

Osumilite is a cyclosilicate constituent of the major minerals observed in the XRD of the biochar samples as presented in Table 7. Other mineral peaks are cristobalite, muscovite, tridymite, stannite, chaoite, and sanidine. It has

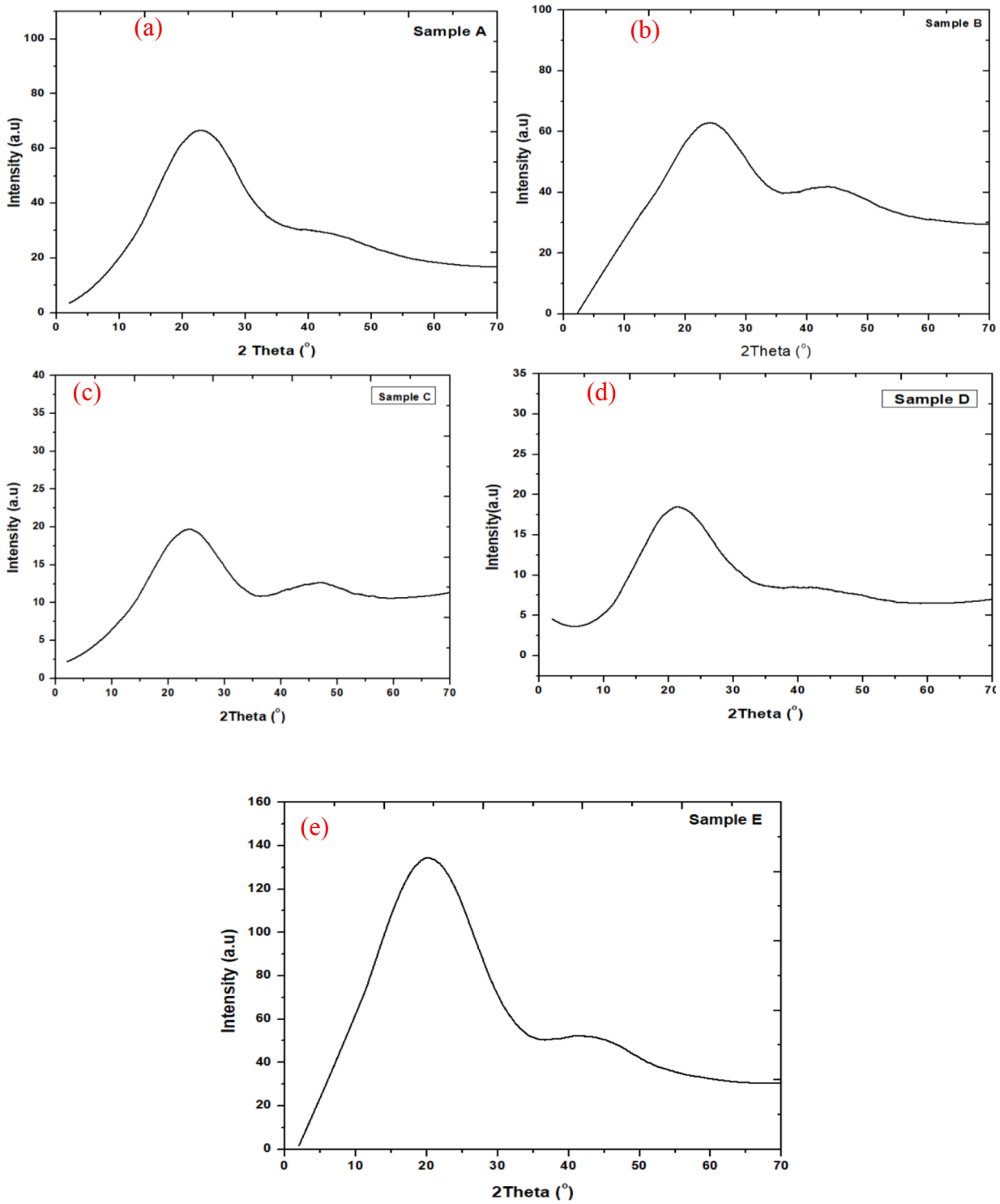

Fig. 12 XRD for the samples

been reported that an amorphous and crystalline cellulose structure is obtainable at peaks between 16 and 25 for biomass [58, 59]. However, the pyrolysis temperature increase caused the disappearance of these peaks. This implied that the presence of cellulose is degraded and the organic compounds are volatilized [58].

In a study by Gale et al. [60], it was reported based on XRD analysis that there is a surface area increment as the heating temperature increases leading to the breaking down

Table 7 Chemical composition of mineral phases in the biochar samples

Mineral phase	Chemical composition
Silicon oxide	SiO_2
Graphite	C
Osumilite	(K, Na) (Fe, Mg) (Al, Fe)$_3$ (Si, Al)$_{12}O_{30}$
Chlorite	ClO_2^-
Albite	$NaAlSi_3O_8$

Table 8 Functions of the elements in the biochar for soil fertility and plant growth

Element	Function	Reference
K	Essential macronutrient for growth and plant metabolism. Improve draught resistance	[65]
Na	Improves soil structure Reduce erodibility Improves water-holding capacity	[66]
Fe	Formation of chlorophyll in plant cells Activator for biochemical processes in plants	[66]
Mg	Improves soil structure with enhanced aggregation Improves soil holding capacity Essential for photosynthesis Serves as activator for enzymes	[66]
Al	Stimulate root growth Increased nutrient uptake Increase enzyme activity	[67]
Si	Improves soil aggregation and water-holding capacity	[68]
Cl	Required in photosynthetic reaction	[66]
Ni	Prevent toxic accumulation of urea Participate in nitrogen metabolism of legumes Essential for seed development	[66]
Zn	An important plant growth regulator	[66]
Cu	Production of vitamin A Activator of many enzymes in plant	[66]

of biomass constituents. Hemicellulose is known to degrade first before cellulose due to the high resistance of cellulose to hydrolysis compared to hemicellulose. The degradation of biomass when subjected to further thermal treatment may occur via hydrolysis, isomerization, dehydration, and fragmentation [51, 60].

As reported by a study, after various combustion technologies, the existence of cristobalite, quartz, and tridymite in biomass boosted crystallinity. The catalytic performance of a material is significantly enhanced with the high crystallinity of the biomass material [61]. Similar peaks observed in this present study were reported in the study of Waqas et al. [44]. Biochar production between 300 and 500^oC temperature range had a significant effect on changing the mineralogical constituents of biochar [51, 62–64].

The chemical composition of the mineral phases available in the biochar samples when compared to the element contained in EDX spectra of the biochar samples confirmed the elements present. The elements present in the biochar tend to assist in soil fertilization.

The various functions of the element present in the biochar are displayed in Table 8.

4 Conclusion

Bio-oil and biochar from the pyrolysis and co-pyrolysis of biomass (sawdust) and plastic waste (PET bottles) were successfully produced using an ablative pyrolyzer and characterized. The highest bio-oil and biochar yields are 51.33 g (100% PET) and 22.82% (100% Sawdust), respectively. Hence, the more the bio-oil obtained, the lower the biochar yield and vice versa. With the values obtained for density, pour point, cloud point, viscosity, and pH of the bio-oil, it would require further processes to be useful as biofuel. The microstructure of the biochar showed fibrous rigid structures with numerous pores, especially for the biochar samples with up to 50% plastic waste. However, the microstructure of the biochar samples with 75% and 100% plastic wastes revealed minimal pores due to clogging of the plastics after carbonization. The bio-oil samples contain alcohols, acids, and esters based on the FTIR analysis. The XRD pattern revealed different mineral phases such as silicon oxide, graphite, osumilite, chlorite, and albite. These mineral phases contain both major and minor elements which can be useful for soil improvement and some other applications. It is recommended that for energy applications and utilizations, further chemical processes should be carried out on the bio-oil obtained. It is suggested that further investigations should be done on the kinetics of the two combined samples, which would enhance the comprehension of the energy potential of the substrates in the near future.

Acknowledgements The author appreciates the Management of Landmark University for providing a conducive environment to carry out this study. The assistance rendered during the experimentation stage by the technician in the Energy Laboratory, Department of Mechanical Engineering, Landmark University, Nigeria is appreciated.

Author Contributions Peter Ikubanni and Adekunle Adeleke conceived and designed the study. Funding acquisition and resources were by Peter Ikubanni, Ayotomiwa Adedayo, Uchechukwu Robinson, and Olayinka Agboola. Material preparation, Data collection, and analysis were performed by Peter Ikubanni, Adekunle Adeleke, Ayotomiwa Adedayo, Uchechukwu Robinson, Deborah Danjuma, Timothy Adekanye, and Oluwasogo Ogundipe. The first draft of the manuscript was written by Peter Ikubanni. All other authors contributed by reviewing and editing the first draft. All authors read and approved the final version to be published.

Data Availability Data associated with the manuscript are available on request from the authors.

Declarations

Conflict of Interest The authors have no relevant financial or non-financial interests to disclose.

References

1. Saleem M, Baig N (2018) Production of bio-oil and bio-char from different biomass wastes. IOP Conf Series: Mat Sci Eng 458(1). https://doi.org/10.1088/1757-899X/458/1/012021
2. Varma A (2016) Physicochemical characterization and pyrolysis kinetics of wood sawdust. Ener Sour Part A: Recov Utiliz Environ Eff 38:2536–2544. https://doi.org/10.1080/15567036.2015.1072604
3. Alabdrabalnabi A, Gautam R, Sarathy SM (2022) Machine learning to predict biochar and bio-oil yields from co-pyrolysis of biomass and plastic. Fuel 328:125303. https://doi.org/10.1016/j.fuel.2022.125303
4. Irena (2014) Renewable power generation costs in 2014. Accessed 23 June 2023
5. Trinh QT, Banerjee A, Ansari KB, Dao DQ, Drif A, Binh NT, Tung DT, Binh PMQ, Amaniampong PN, Huyen PT, Le MT (2020) Upgrading of bio-oil from biomass pyrolysis: current status and future development. In: Nanda S, Vo D-VN, Sarangi PK (eds) Biorefinery of Alternative resources: Targeting Green fuels and platform chemicals. Springer, Singapore, pp 317–353. https://doi.org/10.1007/978-981-15-1804-1_14
6. Inayat A, Ahmed A, Tariq R, Waris A, Jamil F, Ahmed SF, Ghenai C, Park YK (2022) Techno-economical evaluation of bio-oil production via biomass fast pyrolysis process: a review. Front Ener Res 9:1–9. https://doi.org/10.3389/fenrg.2021.770355
7. Boran FE (2018) A new approach for evaluation of renewable energy resources: a case of Turkey. Ener Sour B: Econ Plan Pol 13:196–204. https://doi.org/10.1080/15567249.2017.1423414
8. Okolie JA, Jimoh T, Akande O, Okoye PU, Ogbaga CC, Adeleke AA, Ikubanni PP, Gulec F, Amenaghawon AN (2023) Pathways for the valorization of animal and human waste to biofuels, sustainable materials and value-added chemicals. Environments 10(46):1–38. https://doi.org/10.3390/environments10030046
9. Ibikunle RA, Titiladunayo IF, Akinnuli BO, Lukman AF, Ikubanni PP, Agboola OO (2018) Modelling the energy content of municipal solid waste and determination of its physico-chemical correlation using multiple regression analysis. Int J Mech Eng Technol 9(11):220–232
10. Adeleke AA, Ikubanni PP, Orhadahwe TA, Christopher CT, Akano JM, Agboola OO, Adegoke SO, Balogun AO, Ibikunle RA (2021) Sustainability of multifaceted usage of biomass: A review. Heliyon 7 (e08025). https://doi.org/10.1016/j.heliyon.2021.308025
11. Adeleke AA, Odusote JK, Ikubanni PP, Lasode OA, Malathi M, Paswan D (2021b) Essential basics on biomass torrefaction, densification and utilization. Int J Ener Res 45(2):1375–1395. https://doi.org/10.1002/er.5884
12. Chen D, Yin L, Wang H, He P (2014) Pyrolysis technologies for municipal solid waste: a review. Waste Manage 34:2466–2486. https://doi.org/10.1016/j.wasman.2014.08.004
13. Mariyam S, Alherbawi M, Rashid N, Al-Ansari T, McKay G (2022) Bio-oil production from multi-waste biomass co-pyrolysis using analytical Py–GC/MS. Energies 15:7409. https://doi.org/10.3390/en15197409
14. Gupta S, Mondal P, Borugadda VB, Dalai AK (2021) Advances in upgradation of pyrolysis bio-oil and biochar towards improvement in bio-refinery economics: a comprehensive review. Environ Technol Innov 21:101276. https://doi.org/10.1016/j.eti.2020.101276
15. Adeleke AA, Odusote JK, Ikubanni PP, Lasode OA, Malathi M, Paswan D (2020) The ignitability, fuel ratio and ash fusion temperature of torrefied woody biomass. Heliyon 6(3):e03582. https://doi.org/10.1016/j.heliyon.2020.e03582
16. Isikgor FH, Becer CR (2015) Lignocellulosic biomass: a sustainable platform for the production of bio-based chemicals and polymers. Polym Chem 6:4497–4559. https://doi.org/10.1039/c5py00263j
17. Zhang Q, Chang J, Wang T, Xu Y (2007) Review of biomass pyrolysis oil properties and upgrading research. Ener Conv Manage 48:87–92. https://doi.org/10.1016/J.enconman.2006.05.010
18. Abnisa F, Wan Daud WMA (2014) A review on co-pyrolysis of biomass: an optional technique to obtain a high-grade pyrolysis oil. Ener Conv Manage 87:71–85. https://doi.org/10.1016/J.enconman.2014.07.007
19. Khan MZH, Sultana M, Al-Mamun MR, Hasan MR (2016) Pyrolytic waste plastic oil and its diesel blend: fuel characterization. J Environ Public Health 2016:1–6. https://doi.org/10.1155/2016/7869080
20. Egbosiuba TS (2022) Biochar and bio-oil properties from nickel nanoparticles assisted pyrolysis of cassava peel. Heliyon 8:e10114. https://doi.org/10.1016/j.heliyon.2022.e10114
21. Tang Y, Ma X, Lai Z (2011) Thermogravimetric analysis of the combustion of microalgae and microalgae blended with waste in N_2/O_2 and CO_2/O_2 atmospheres. Biores Technol 102:1879–1885. https://doi.org/10.1016/j.biortech.2010.07.088
22. Dorado C, Mullen CA, Boateng AA (2015) Origin of carbon in aromatic and olefin products derived from HZSM-5 catalyzed co-pyrolysis of cellulose and plastics via isotopic labeling. Appl Catal B 162:338–345. apcatb.2014.07.006 https://doi.org/10.1016/j.apcatb.2014.07.006
23. Struhs E, Sotoudehnia F, Mirkouei A, McDonald AG, Ramirez-Corredores M (2022) Effect of feedstocks and free-fall pyrolysis on bio-oil and biochar attributes. J Anal Appl Pyroly 166:105616. https://doi.org/10.1016/j.jaap.2022.105616
24. Zhang H, Chen C, Gray EM, Boyd SE (2017) Effect of feedstock and pyrolysis temperature on properties of biochar governing end-use efficacy. Biomass Bioener 105:136–146. https://doi.org/10.1016/j.biombioe.2017.06.024
25. Adegoke SO, Adeleke AA, Ikubanni PP, Falode AO, Alawode AJ, Agboola OO, Adediran AA (2021) Design and fabrication of an ablative pyrolyser for production bio-lubricants and chemicals in oil well drilling application. IOP Conf Series: Earth Environ Sci 665:012007. https://doi.org/10.1088/1755-1315/665/1/012007
26. Pandey U, Stormyr JA, Hassani A, Jaiswal R, Haugen HH, Moldestad BME (2020) Pyrolysis of plastic waste to environmentally friendly products. WIT Trans Ecol Environ 246:61–74. https://doi.org/10.2495/EPM200071
27. Fogarassy C, Toth L, Czikkely M, Finger DC (2019) Improving the efficiency of pyrolysis and increasing the quality of gas production through optimization of prototype systems. Resources 8(4). https://doi.org/10.3390/resources8040182
28. Yin R, Liu R, Mei Y, Fei W, Sun X (2013) Characterisation of bio-oil and bio-char obtained from sweet sorghum bagasse fast pyrolysis with fractional condenser. Fuel 112:96–104. https://doi.org/10.1016/j.fuel.2013.04.090
29. Trubetskaya A, von Berg L, Johnson R, Moore S, Leahy JJ, Han Y, Lange H, Anca-Couce A (2023) Production and characterization of bio-oil from fluidized bed pyrolysis of olive stones, Pinewood, and torrefied feedstock. J Analy Appl Pyrol 169:105841. https://doi.org/10.1016/j.jaap.2022.105841
30. Shariff A, Aziz NSM, Ismail NI, Abdullah N (2016) Corn cob as a potential feedstock for slow pyrolysis of biomass. J Phys Sci 27(2):123–137. https://doi.org/10.21315/jps2016.27.2.9

31. Adegoke SO, Falode AO, Adeleke AA, Ikubanni PP, Agboola OO (2020) Production of an alternative fuel for drilling industry from a blend of polypropylene wastes and Jatropha distillates. AIMS Ener 8(6):1127–1142. https://doi.org/10.3934/energy.2020.6.1127
32. Aboelela D, Saleh H, Attia A, Elhenawy Y, Majozi T, Bassyouni M (2023) Recent advances in biomass pyrolysis processes for bioenergy production: optimization of operating conditions. Sustainability 15(14):11238. https://doi.org/10.3390/su151411238
33. Choi JH, Kim SS, Suh DJ, Jang EJ, Min KI, Woo HC (2016) Characterization of bio-oil and biochar produced by fixed bed pyrolysis of the brown alga *Saccharina Japonica*. Korean J Chem Eng 33:2691–2698. https://doi.org/10.1007/s11814-016-0131-5
34. Adeleke AA, Odusote JK, Ikubanni PP, Orhadahwe TA, Lasode OA, Ammasi A, Kumar K (2021c) Ash analyses of Bio-coal briquettes produced using blended Binder. Sci Rep 11(1):547. https://doi.org/10.1038/s41598-020-79510-9
35. Clemente-Castro S, Palma A, Ruiz-Montoga M, Giraldez I, Diaz MJ (2023) Optimizing pyrolysis parameters and product analysis of a fluidized bed pilot plant for *Leucaena leucophila* biomass. Envirn Sci Europe 35:1–20. https://doi.org/10.1186/s12302-023-00800-w
36. Zhang L, Bao Z, Xia S (2018) Catalytic pyrolysis of biomass and polymer wastes. Catalyst 8:1–45. https://doi.org/10.3390/catal8120659
37. Chukwuneke JL, Ewulowu MC, Chuwujike IC, Okolie PC (2019) Physico-chemical analysis of pyrolyzed bio-oil from *Swietenia macrophylla* (mahogany) wood. Heliyon 5:e01790. https://doi.org/10.1016/j.heliyon.2019.e01790
38. Anandaram H, Srivastava BP, Vijayakumar B, Madhu P, Depoures MV, Patil PP, Chhabria S, Patel PB, Prabhakar S (2022) Co-pyrolysis characteristics and synergestic interaction of waste polyethylene terephthalate and woody biomass towards bio-oil production. J Chem 2022:3699076. https://doi.org/10.1155/2022/3699076
39. Garba MU, Musa U, Olugbenga AG, Mohammad YS, Yahya M, Ibrahim AA (2018) Catalytic upgrading of bio-oil from bagasse: thermogravimetric analysis and fixed bed pyrolysis. Beni-Suef Univ J Basic Appl Sci 7:776–781. https://doi.org/10.1016/j.bjbas.2018.11.004
40. Wijayanti H, Irawan C, Aulia N (2022a) Copyrolysis of rice husk and plastic bags waste from low-density polyethylene (LDPE) for improving pyrolysis liquid product. IOP Conf Series: Earth Environ Sci 963:012012. https://doi.org/10.1088/1755-1315/963/1/012012
41. Wijayanti W, Musyaroh M, Sasongko MN (2022b) Low-density polyethylene plastic waste to liquid fuel using pyrolysis method: an effect of temperatures on the oil yields physicochemical properties. J Sustain Dev Ener Water Environ Sys 10(3):1–18. https://doi.org/10.13044/j.sdewes.d9.0402
42. Eyankware EO, Ulakpa WC, Eyankware MO (2016) Determination of cloud and pour point of crude oil with reference to crude transportation. Int J Sci Healthc Res 1(3):20–28
43. Cárdenas–Zapata R, Palma-Ramírez D, Flores-Vela AI, Romero–Partida JN, Paredes-Rojas JC, Marquez-Rocha FJ, Bravo-Díaz B (2022) Structural and thermal study of hemicellulose and lignin removal from two types of sawdust to isolate cellulose. MRS Adv 7:49–55. https://doi.org/10.1557/s43580-022-00225-2
44. Chen H (2014) Chemical composition and structure of natural lignocellulose. Biotechnology of lignocellulose. Springer, Dordrecht. pp https://doi.org/10.1007/978-94-007-6898-7_2
45. Li P, Shi X, Wang X, Song J, Fang S, Bai J, Zhang G, Chang C, Pang S (2021) Bio-oil from biomass fast pyrolysis: yields, related properties and energy consumption analysis of the pyrolysis system. J Clean Prod 328:129613. https://doi.org/10.1016/j.jclepro.2021.129613
46. Ozcimen D, Karaosmanoglu F (2004) Production and characterization of bio-oil and biochar from rapeseed cake. Renew Energy 29:779–787. https://doi.org/10.1016/j.renene.2003.09.006
47. Solikhah M, Pratiwi F, Heryana Y, Wimada A, Karuana F, Raksodewanto A, Kismanto A (2018) Characterization of bio-oil from fast pyrolysis of palm frond and empty fruit bunch. IOP Conf Series: Mat Sci Eng 349:012035. https://doi.org/10.1088/1757-899X/349/1/012035
48. Le PT, Bui HT, Le DN, Nguyen TH, Pham LA, Nguyen HM, Nguyen QS, Nguyen TP, Bich NT, Duong TT, Herrmann M, Ouillon S, Le TPQ (2021) Preparation and characterization of biochar derived from agricultural by-products for dye removal. Adsorp Sci Technol 2021:9161904. https://doi.org/10.1155/2021/9161904
49. Ma X, Zhou B, Budai A, Jeng A, Hao X, Wei D, Zhang D, Rasse D (2016) Study of biochar properties by scanning electron microscope– energy dispersive x-ray spectroscopy (SEM-EDX). Commun Soil Sci Plant Analy 47(5):593–601. https://doi.org/10.1080/00103624.2016.1146742
50. Ghani WAWAK, Mohd A, da Silva G, Bachmann RT, Taufiq-Yap YH, Rashid U, Ala'a H (2013) Biochar production from waste rubber-wood-sawdust and its potential use in C sequestration: Chemical and physical characterization. Ind Crops Prod 44:18–24. https://doi.org/10.1016/j.indcrop.2012.10.007
51. Waqas M, Aburiazaiza AS, Minadad R, Rehan M, Barakat MA, Nizami AS (2018) Development of biochar as fuel and catalysts in energy recovery technologies. J Clean Prod 188:477–488. https://doi.org/10.1016/j.clepro.2018.04.017
52. Ikubanni PP, Oki M, Adeleke AA, Adediran AA, Adesina OS (2020) Influence of temperature on the chemical compositions and microstructural changes of ash formed from palm kernel shell. Res Eng 8(100373). https://doi.org/10.1016/j.rineng.2020.100173
53. Ikubanni PP, Oki M, Adeleke AA, Adesina OS, Omoniyi PO (2021a) Physico-tribological characteristics and wear mechanisms of hybrid reinforced Al6063 matrix composites. Acta Metallur Slovaca 27(4):172–179. https://doi.org/10.36547/ams.27.4.1084
54. Ikubanni PP, Oki M, Adeleke AA, Omoniyi PO (2021b) Synthesis, physico-mechanical and microstructural characterization of Al6063/SiC/PKSA hybrid reinforced composites. Sci Rep 11(14845):1–13. https://doi.org/10.1038/s42598-021-94420-0
55. Ikubanni PP, Oki M, Adeleke AA, Omoniyi PO, Ajisegiri ESA, Akinlabi E (2022) Physico-mechanical properties and microstructure responses of hybrid reinforced Al6063 composites to PKSA/SiC inclusion. Acta Metallur Slovaca 28(1):25–32. https://doi.org/10.36547/ams.28.1.1340
56. Wu W, Yang M, Feng Q, McGrouther K, Wang H, Lu H, Chen Y (2012) Chemical characterization of rice straw-derived biochar for soil amendment. Biom Bioener 47:268–276. https://doi.org/10.1016/j.biombioe.2012.09.034
57. Shaaban A, Se SM, Dimin M, Juoi JM, Husin MHM, Mitan NMM (2014) Influence of heating temperature and holding time on biochars derived from rubber wood sawdust via slow pyrolysis. J Anal App Pyroly 107:31–39. https://doi.org/10.1016/j.jaap.2014.01.021
58. Hadey C, Allouch M, Alami M, Boukhlifi F, Loulidi I (2022) Preparation and characterization of biochar obtained from biomasses for combustible briquette application. Sci World J 2022(2554475). https://doi.org/10.1155/2022/2554475
59. Sahoo SS, Vijay VK, Chandra R, Kumar H (2021) Production and characterization of biochar produced from slow pyrolysis of pigeon pea stalk and bamboo. Clean Eng Technol 3(100101). https://doi.org/10.1016/j.clet.2021.100101
60. Gale M, Nguyen T, Moreno M, Gilliard-AbdulAziz KL (2021) Physiochemical properties of biochar and activated carbon from biomass residues: influence of process conditions to

adsorbent properties. ACS Omega 6(15):10224–10233. https://doi.org/10.1021/acsomega.1c00530
61. Hossain N, Nizamuddin S, Griffin G et al (2020) Synthesis and characterization of rice husk biochar via hydrothermal carbonization for wastewater treatment and biofuel production. Sci Rep 10(18851). https://doi.org/10.1038/s41598-020-75936-3
62. Ahmad M, Ahmad M, Usman AR, Al-Faraj AS, Abduljabbar A, Ok YS, Al-Wabel MI (2017) Date palm waste-derived biochar composites with silica and zeolite: synthesis, characterization and implication for carbon stability and recalcitrant potential. Environ Geochem Health 41:1687–1704. https://doi.org/10.1007/s10653-017-9947-0
63. Yuan JH, Xu RK, Zhang H (2011) The forms of alkalis in the biochar produced from crop residues at different temperatures. Bioresour Technol 102(3):3488–3497. https://doi.org/10.1016/j.biortech.2010.11.018
64. Ding Z, Wan Y, Hu X, Wang S, Zimmerman AR, Gao B (2016) Sorption of lead and methylene blue onto hickory biochars from different pyrolysis temperatures: importance of physicochemical properties. Ind Eng Chem Res 37:261–267. https://doi.org/10.1016/j.jiec.2016.03.035
65. Rawat J, Sanwal P, Saxena J (2016) Potassium and its role in sustainable agriculture. In: Meena V, Maurya B, Verma J, Meena R (eds) Potassium solubilizing microorganisms for sustainable agriculture. Springer, New Delhi, pp 235–253. https://doi.org/10.1007/978-81-322-2776-2_17
66. Manjula VN (2017) Soils, plant nutrition and nutrient management. Master Gardener, Chap. 4, 1–12. https://extension.missouri.edu/publications/mg4 Accessed 18 August 2023
67. Bojórquez-Quintal E, Escalante-Magaña C, Echevarría-Machado I, Martínez-Estévez M (2017) Aluminum, a friend or foe of higher plants in acid soils. Front Plant Sci 8:1767. https://doi.org/10.3389/fpls.2017.01767
68. Tubana BS, Babu T, Datnoff LE (2016) A review of silicon in soils and plants and its role in agriculture: history and future perspectives. Soil Sci 181:393–411. https://doi.org/10.1097/SS.0000000000000179